

Figure S1. Seismic properties of the olivine aggregates in the (a and b) MEC and (c–g) FEC and (h) olivine single crystal at ambient condition. Data are presented in an equal area and upper hemisphere stereonets. First column: P-wave velocity (V_p) and its anisotropy (AV_p); second column: shear wave splitting or S-wave polarization anisotropy (AV_s) and its maximum (max. AV_s); third column: fast S-wave velocity (V_{s1}) and its anisotropy (AV_{s1}). Black bars in the V_{s1} stereonets indicate the polarization directions of the fast shear wave. X , Y , and Z denote the lineation, direction perpendicular to the lineation and parallel to the foliation, and foliation-normal direction, respectively. X' and Y' are the apparent lineation and the direction perpendicular to the lineation on the apparent foliation ($X'Y'$ plane).

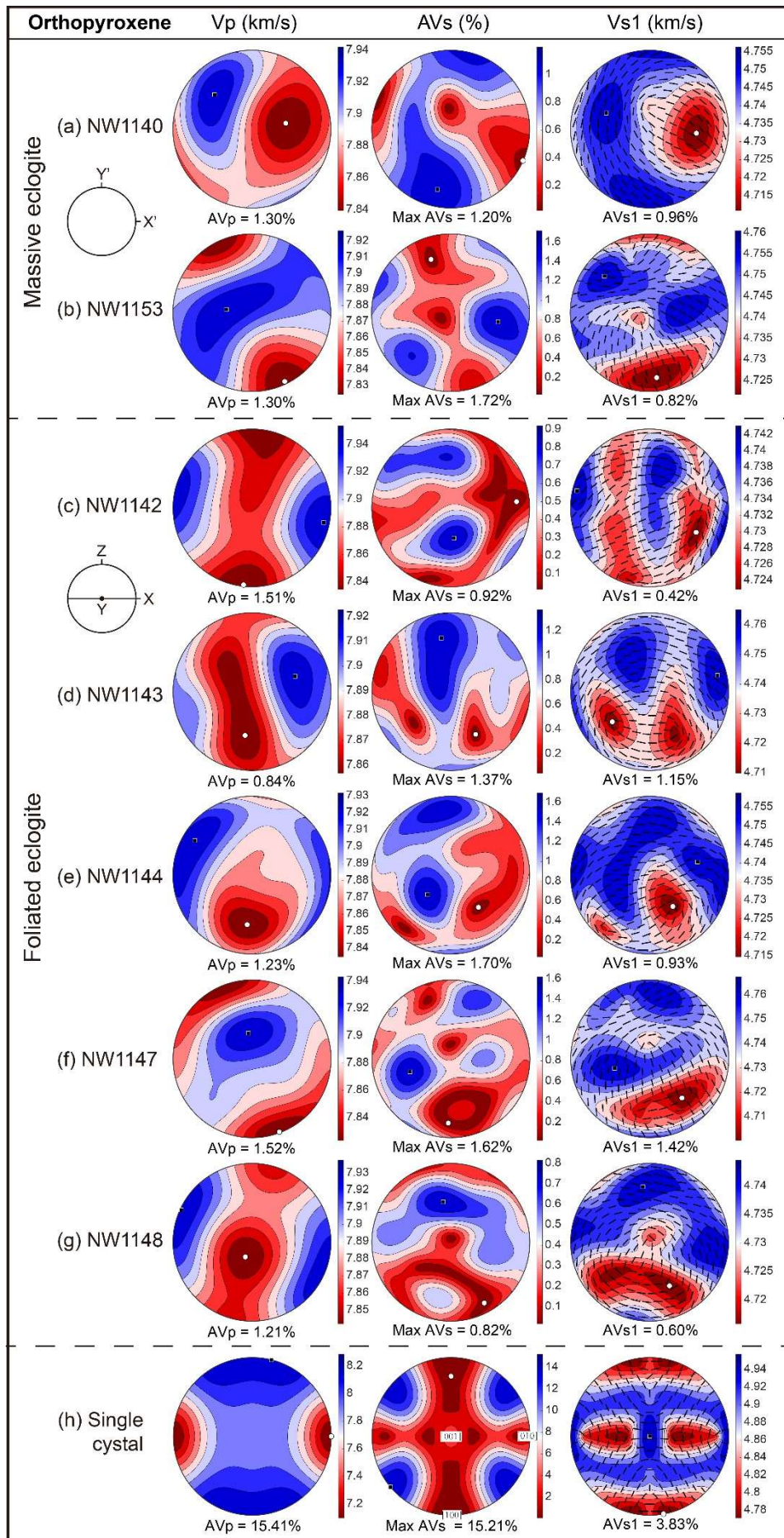


Figure S2. Seismic properties of the orthopyroxene aggregates in the (a and b) MEC and (c–g) FEC and (h) orthopyroxene single crystal at ambient condition. Legends are the same as Fig. S1.

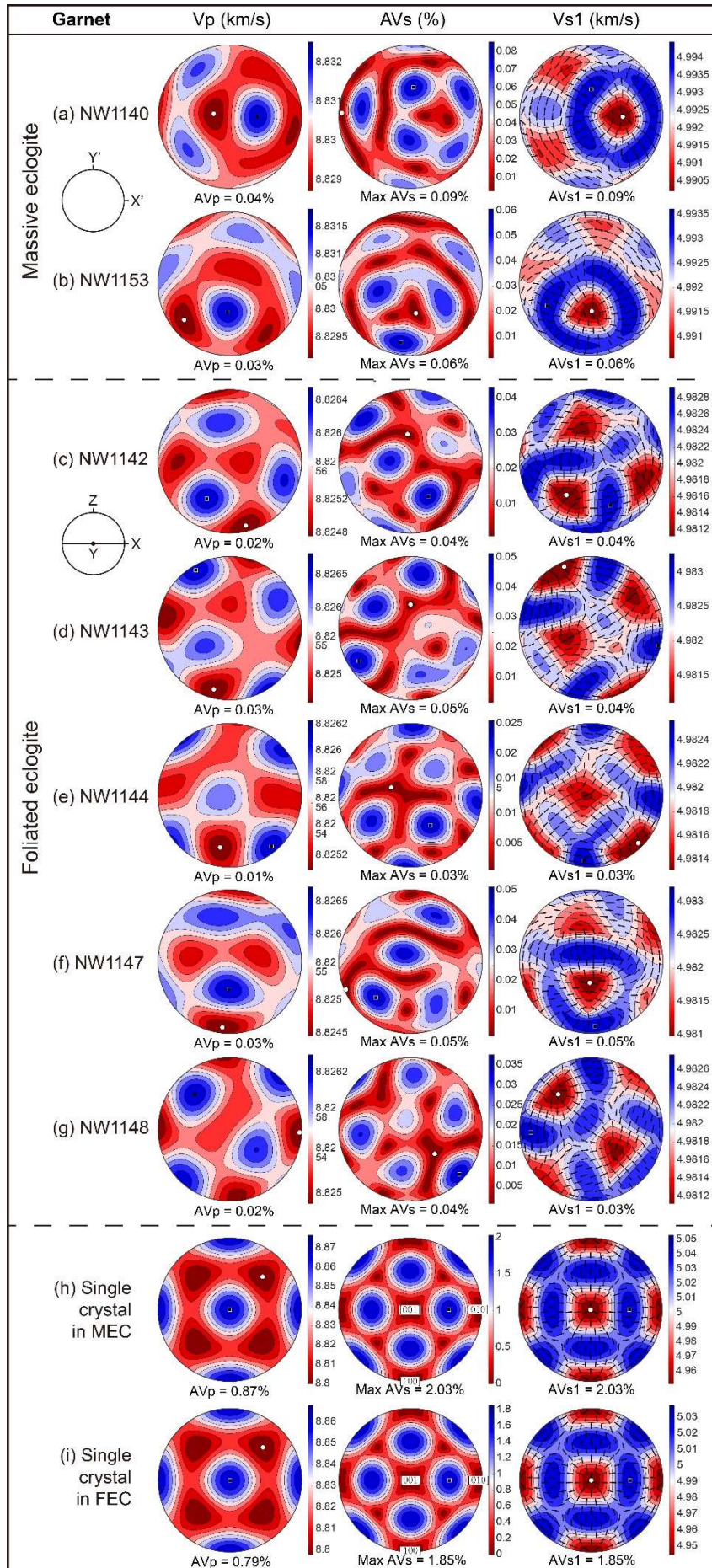


Figure S3. Seismic properties of the garnet aggregates in the (a and b) MEC and (c–g) FEC and garnet single crystals in (h) MEC and (i) FEC at ambient condition. Legends are the same as Fig. S1.

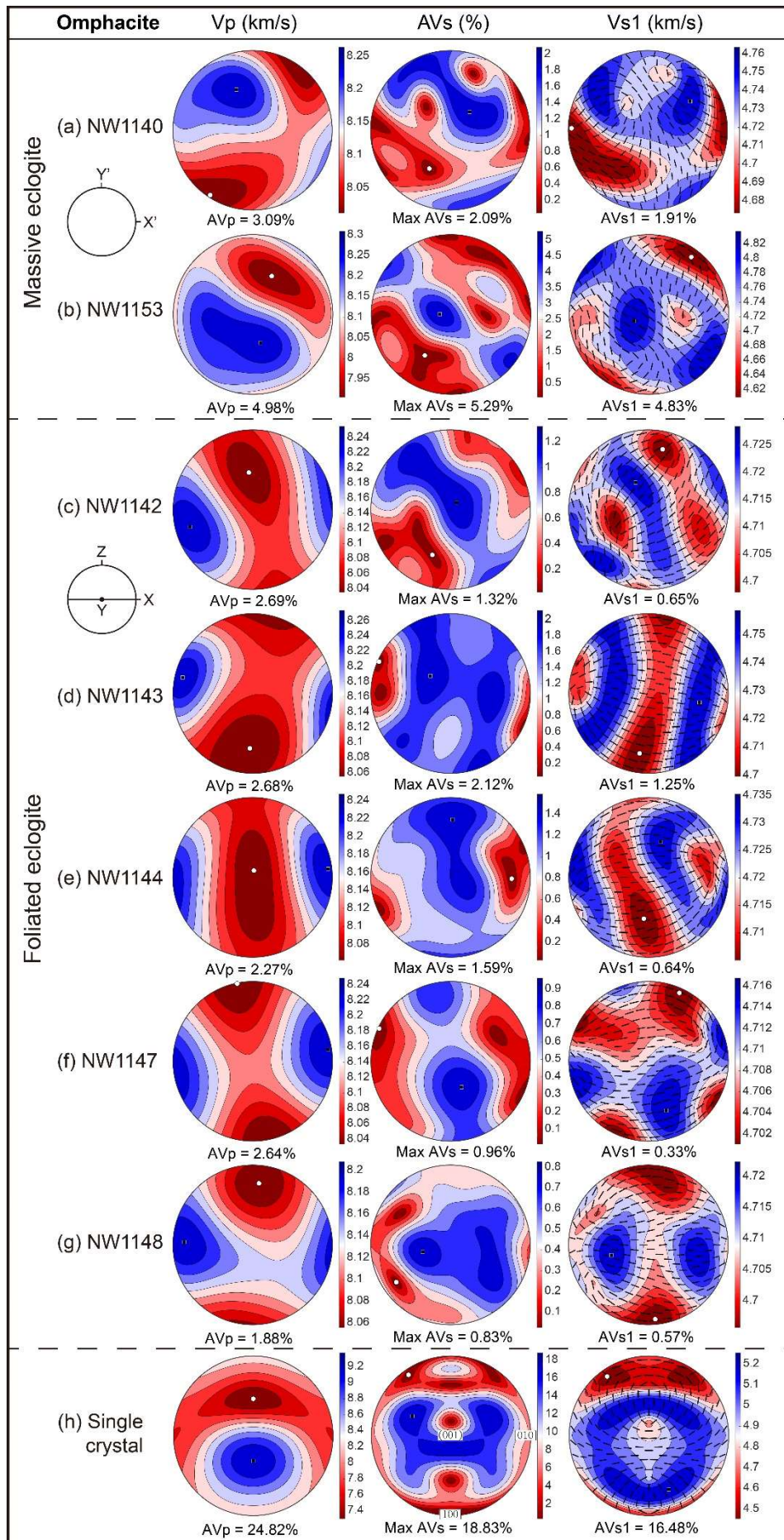


Figure S4. Seismic properties of the omphacite aggregates in the (a and b) MEC and (c–g) FEC and (h) omphacite single crystal at ambient condition. Legends are the same as Fig. S1.

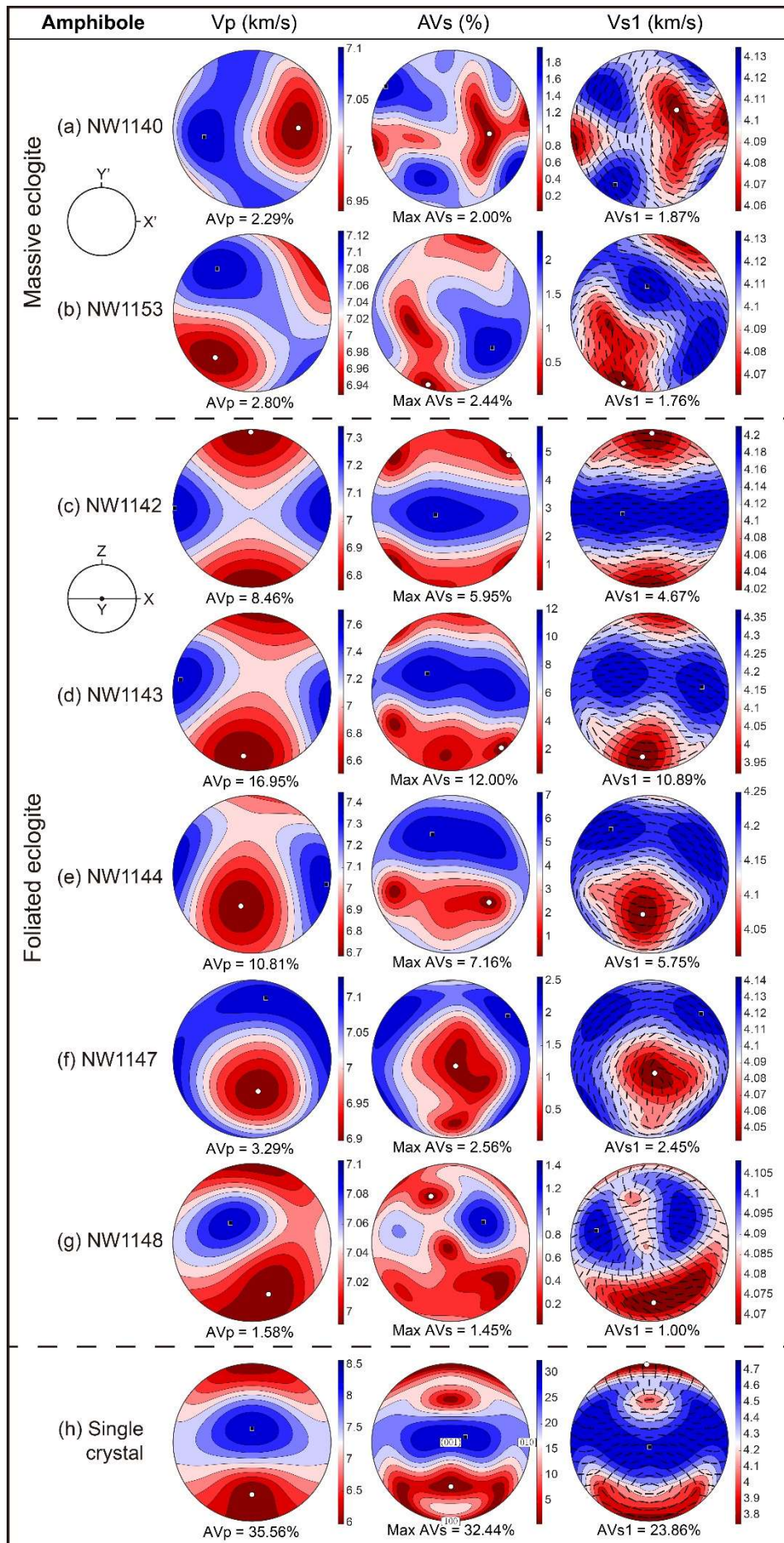


Figure S5. Seismic properties of the amphibole aggregates in the (a and b) MEC and (c–g) FEC and (h) amphibole single crystal at ambient condition. Legends are the same as Fig. S1.